HYDROLOGICAL PROCESSES
Hydrol. Process. **14**, 497–519 (2000)

Flood inundation simulation in a river basin using a physically based distributed hydrologic model

Dushmanta Dutta,[1]* Srikantha Herath[1] and Katumi Musiake[2]
[1]*INCEDE, IIS, The University of Tokyo, 7-22-1 Roppongi, Minato-ku, Tokyo 106-8558, Japan*
[2]*IIS, The University of Tokyo, 7-22-1 Roppongi, Minato-ku, Tokyo 106-8558, Japan*

Abstract:

A physically based distributed hydrologic model is developed in this study for flood inundation simulation combining newly developed overland and channel network flow simulation models with evapotranspiration, unsaturated zone and saturated zone models. The overland flow and river flow models are validated individually with test data, and then coupled with other models. The model can take fine resolution spatial data as input preserving spatial heterogeneity of physical characteristics of a river basin. River embankments play an important role in flood prevention. The model can incorporate river embankment data in flood inundation simulation. The model is applied in a river catchment in Japan to simulate a flood event in 1996. Outputs from the model show good agreements with observed flood hydrographs and surveyed flood inundation. Copyright © 2000 John Wiley & Sons, Ltd.

KEY WORDS distributed hydrologic model; simulation of flood inundation; Ichinomiya river basin

INTRODUCTION

Accurate spatial and temporal information of a flood event are of the utmost importance for various structural and non-structural measures for flood disaster mitigation as well as for flood damage estimation. Physically based hydrologic modelling is an effort to obtain spatial and temporal variation of floodwater by flood inundation simulation.

Various hydrologic models have been developed in the past to simulate flood inundation (Iwasa and Inoue, 1982; Samules, 1985; Gee *et al.*, 1990). However, such models consider only overland and river flows; other components of the hydrologic cycle such as evaporation, unsaturated zone and saturated zone flows are neglected. In real situations, evaporation, infiltration and base flow to a river before a flood event have a significant impact on the occurrence or non-occurrence of floods due to rainfall. Also, these models are applied either only in test catchments or in some small flat areas with hypothetical conditions. Only a few models are available to simulate flood inundation in a river basin for real flood events considering all the spatial heterogeneity of physical characteristics of topography such as HEC, MIKE 11, etc. However, these models are also restricted to overland and river components.

A physically based distributed hydrologic model is a mathematical representation of all the components of hydrologic cycle based on their physical governing equations that can be used to simulate movement of water in different components of the hydrologic cycle in a river basin. There are five major components of a distributed hydrologic model; (i) interception and evapotranspiration, (ii) overland flow, (iii) river flow, (iv) subsurface flow and (v) ground water flow. Figure 1 shows a schematic diagram of a distributed hydrologic

* Correspondence to: Dr D. Dutta, INCEDE, IIS, The University of Tokyo, 7-22-1 Roppongi, Minato-ku, Tokyo 106-8558, Japan.
E-mail: dutta@incede.iis.u-tokyo.ac.jp

CCC 0885–6087/2000/030497–23$17·50

Received 1 December 1998
Accepted 15 February 1999

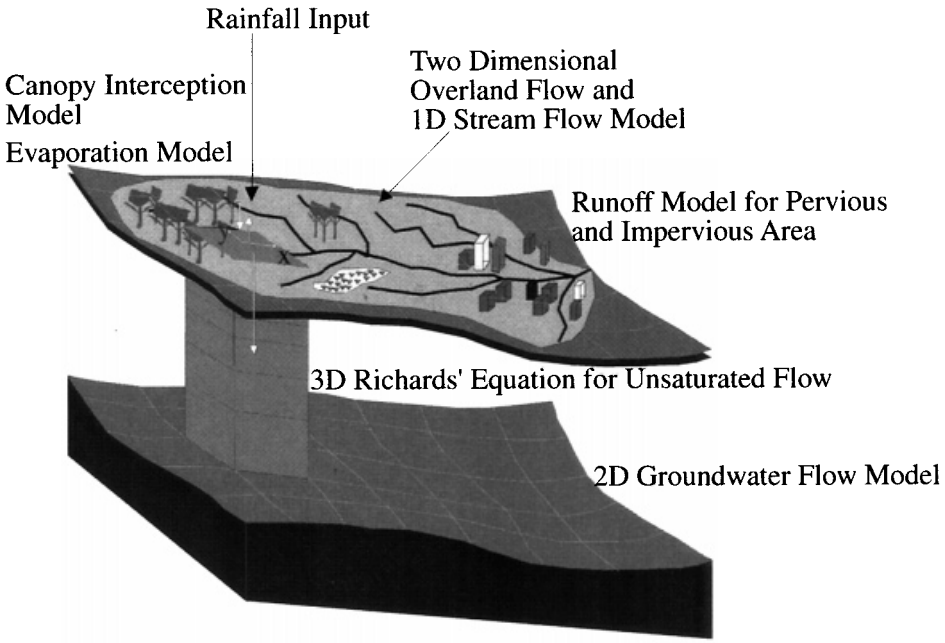

Figure 1. A schematic diagram of a distributed hydrologic model

model. There are already several distributed hydrologic models available which have been developed by various researchers or research organizations for different purposes such as the SHE model, TOPMODEL, WATFLOOD (http://www.hydromodel.com/duan/hydrology), IISDHM (Jha *et al.*, 1997), etc. However, none of these models can simulate flood inundation accurately, mainly due to the limitations in overland and river flow components and their coupling, which are the most important components in flood inundation simulation.

In this study, a coupled mathematical model is developed for overland flow and open channel network flow simulation and it is integrated with the evapotranspiration, unsaturated zone and saturated zone components of IISDHM, a distributed hydrologic model developed at the authors' laboratory. The one-dimensional (1D) open channel flow simulation and two-dimensional (2D) overland flow simulation models are developed using diffusive wave approximation of Saint Venant's equations. The overland flow and river flow models are initially validated individually with test data, and then coupled to consider the exchange of water between surface and river taking into consideration the heights of river embankments. IISDHM solves the evapotranspiration component using the Kristensen and Jensen model, unsaturated zone by the 3D Richard's equation and groundwater flow by the 2D non-linear Boussinesq equation. Finally, these three components of IISDHM are integrated with the newly developed coupled surface and river flow model to develop a complete physically based distributed model. The complete distributed hydrologic model is applied to a river basin in Japan to simulate a flood event of 1996. GIS is used to perform the pre- and post-processing of large amounts of spatial input data and output results efficiently. The results indicate that the model is suitable for basin scale flood inundation simulation considering the spatial heterogeneity of the physical characteristics of a river basin.

MODEL DEVELOPMENT

There are several existing solution schemes for open channel and overland flow simulation using complete hydrodynamic equations (open channel flow: Rahman and Chaudhry, 1997; Cui and Williams, 1998; Field

et al., 1998; overland flow: Fennema and Chaudhry, 1989; Zhang and Cundy, 1989). However, all these solution schemes are tested in laboratory or, in small areas with very mild slopes. In real situations, microtopography, surface roughness, and soil hydraulic properties vary over distances of centimetres to metres, and they strongly influence runoff characteristics along the hillslope, and hillslope hydrographs. To incorporate the heterogeneity of these physical characteristics of a river basin, it is often necessary to make many assumptions for solving the governing equation of flow. Diffusive wave approximation of Saint Venant's equations is good enough to represent surface and open channel flow in a river basin and with this approximation, the numerical instability of a mathematical model can be avoided in basin scale flood inundation simulation. In this study, both 1D open channel flow simulation and 2D overland flow simulation models are derived using the diffusive wave approximation of Saint Venant's equations. Details of the model development processes are described below.

1D Open channel flow simulation model

The basic concept of the channel network flow simulation model is taken from the Y-channel solution scheme proposed by Akan and Yen (1981), which is modified for large channel networks with any number of connecting channels in converging or diverging junctions in this study.

Governing equations. Gradually varied unsteady flow in open channels can be expressed mathematically by the conservation of mass and momentum equations. These two governing equations for unsteady 1D open channel flows are well known as Saint Venant's equations.
Mass conservation equation (continuity equation);

$$\frac{\partial Q}{\partial x} + \frac{\partial A}{\partial t} = q \tag{1}$$

And the momentum equation;

$$\frac{\partial Q}{\partial t} + \frac{\partial}{\partial x}\left(\frac{Q^2}{A}\right) + g\left(\frac{\partial z}{\partial x} + S_f\right) = 0 \tag{2}$$

Where, t = time; x = distance along the longitudinal axis of the water course; A = cross-sectional area; Q = discharge through A; q = lateral inflow or outflow distributed along the x-axis of the watercourse; g = gravity acceleration constant; z = water surface level with reference to datum; and S_f = friction slope.

The friction slope S_f for turbulent flow can be estimated by Manning's formula as follows:

$$S_f = \frac{n^2 Q|Q|}{A^2 R^{4/3}} \tag{3}$$

Where, n = Manning's roughness coefficient; R = hydraulic radius.

Diffusive wave approximation. In the diffusive wave approximation of Saint Venant's equations, the local and convective acceleration terms in the momentum equation (i.e. the first two terms in Equation (2)) are neglected. Thus, Equation (2) is simplified as

$$S_f = -\frac{\partial z}{\partial x} \tag{4}$$

Combining Equations (2) and (4) yields,

$$Q = \frac{1}{n} A R^{2/3} \frac{-\dfrac{\partial z}{\partial x}}{\left|\dfrac{\partial z}{\partial x}\right|^{1/2}} \tag{5}$$

Finite difference equations. A fully implicit finite difference scheme is used to solve these non-linear partial differential equations. Using forward-difference scheme, Equations (1) and (5) can be expressed as,

$$\frac{A_i^{t+1} - A_i^t}{\Delta t} + \frac{Q_{i+1}^{t+1} - Q_i^{t+1}}{\Delta x} = \frac{q_i^{t+1} + q_i^t}{2} \tag{6}$$

$$Q_i^{t+1} = \frac{1}{n_i} A_i^{t+1} (R_i^{t+1})^{2/3} \frac{\dfrac{z_{i+1}^{t+1} - z_i^{t+1}}{\Delta x}}{\left|\dfrac{z_{i+1}^{t+1} - z_i^{t+1}}{\Delta x}\right|^{1/2}} \tag{7}$$

Since the flow cross-sectional area A and hydraulic radius are known functions of water surface elevation z, substituting Equation (7) in (6), yields an equation with three unknowns in the form of

$$f(z_{i-1}^{t+1}, z_i^{t+1}, z_{i+1}^{t+1}) = 0 \tag{8}$$

For a single channel with N points a set of $N-2$ equations with N unknowns can be written. These can be solved with another two equations obtained from upstream (u/s) and downstream (d/s) boundary conditions. The solution techniques are explained in the latter sections.

Channel network equations. For channel networks, the most important point is the appropriate considerations of hydraulic conditions in converging and diverging channel junctions. Hydraulic conditions at a converging channel junction may be described by the continuity equation as,

$$\sum Q_k = Q_o + \frac{ds}{dt} \tag{9}$$

in which, s = the storage within the junction. The subscript k stands for any one of the in-flowing channels and o represents the out-flowing channel. Junctions have small storage volumes in most open-channel networks for which the term ds/dt in Equation (9) is negligible. Thus, it can be written as,

$$\sum Q_k = Q_o \tag{10}$$

Similarly, the above condition can be derived for diverging channel junctions as follows,

$$Q_i = \sum Q_r \tag{11}$$

in which, subscript i represents the in-flowing channel and r stands for any one of the out-flowing channels.

Using the above condition and u/s and d/s boundary conditions, a sufficient number of equations can be obtained in the channel network for solution, since at converging or diverging junctions the head is the same for all the connecting points of the joining branches.

Network solution algorithm. Simultaneous equations resulting from the finite difference approximation of channel networks can be written in matrix notation as [A]{X} = {B}, where [A] is coefficient matrix, {X} is vector of unknown variable z and {B} is vector of intercept values. The Newton-Raphson iteration method is employed for the solution of the simultaneous non-linear finite difference equations.

Comparison of channel network flow simulation model with other models. In order to test the validity of the diffusive wave model for simulation of flow in open-channel networks, a comparison with the kinematic wave model has been made. In the kinematic wave approximation, the inertia as well as pressure terms of the momentum equation Equation (2) are neglected and thus, the friction slope, S_f, is approximated by the bed slope, S_o. In this approximation, backwater effects of channels are neglected and each channel is treated individually. In the solution scheme of river flow with kinematic wave approximation, computations start from the uppermost channels for which u/s boundary conditions are specified, and progress towards d/s channel by channel in a cascading manner, satisfying the flow continuity requirement at junctions. Along a channel reach the $S_f = S_o$, Equations (1) and (3) are combined to yield,

$$\frac{\partial A}{\partial t} + \frac{\partial}{\partial x}\left(\frac{S_o^{1/2}}{n} AR^{2/3}\right) = 0$$

Comparison of models: A hypothetical example is considered here to demonstrate the validity of the diffusive wave model compared to the kinematic wave model. The example considered here is for a channel network of four channels as shown in Figure 2(a). All four channels are assumed to be rectangular channels. The dimensions of the four channels are listed in Table I. Three inflow hydrographs are considered as u/s boundary conditions for channels 1, 2 and 3 as shown in Figure 2(b). No lateral flow is considered and the initial condition is considered as uniform discharges of five cumec along all four channels. Δx and Δt are considered as 50 m and 10 seconds respectively. Two cases are considered for simulation with two different boundary conditions at the exit of channel 4. In the first simulation, the d/s boundary condition at the exit of channel 4 is specified as a uniform flow equation assuming this channel is hydraulically long. In the second simulation, the d/s boundary is considered as a constant depth at 0·5 m to verify the backwater effect in the diffusive wave model.

The computed discharge hydrographs for both cases of simulation using kinematic and diffusive wave models are shown in Figure 3. The figure shows simulated hydrographs at point A of channel 4 for the two simulations. As can be observed from the simulated hydrographs for the first case, the result of the diffusive-wave model is in good agreement with the result of the kinematic wave model as there is no impact of boundary condition due to consideration of uniform flow in the d/s exit of channel 4 in this case. However, the computed hydrographs from the diffusive and kinematic wave models do not agree for the second simulation case. In this case also, the kinematic wave model gives a similar output to the first case as there is no consideration of the back water effect due to the fixed head boundary condition. But, as the diffusive wave model takes into account the backwater effect by considering friction slope, the fixed head boundary condition has affected the hydrograph at point A in this case. Thus, the simulated results show that the

Table I. Properties of example open-channel network

Channel number	Length (m)	Slope	Width (m)	Depth (m)	Manning's coefficient
1	1220	0·0005	20	6	0·02
2	1220	0·0005	20	6	0·02
3	1000	0·001	20	6	0·02
4	1000	0·001	60	6	0·02

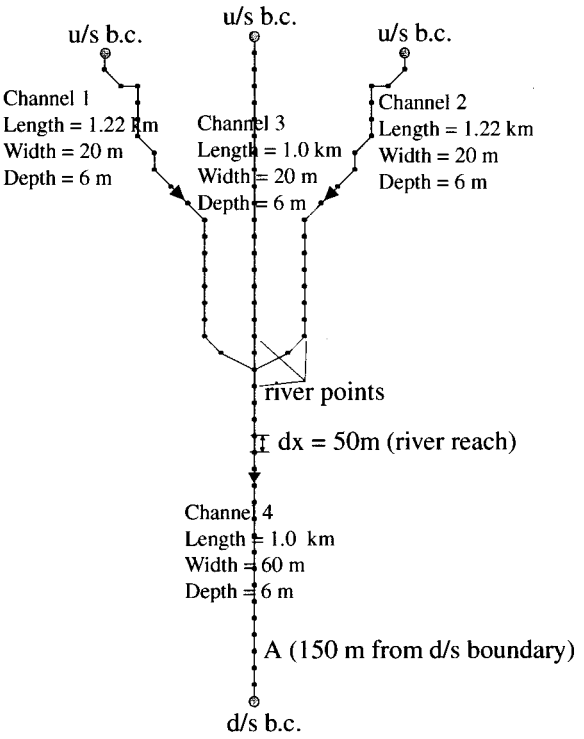

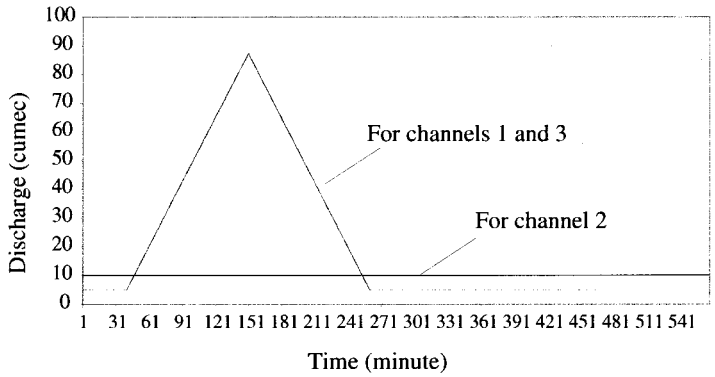

Figure 2. (a) Channel network used for testing of open channel network solution algorithm; (b) input discharge hydrographs in u/s points of channel 1, 2 and 3 as boundary conditions

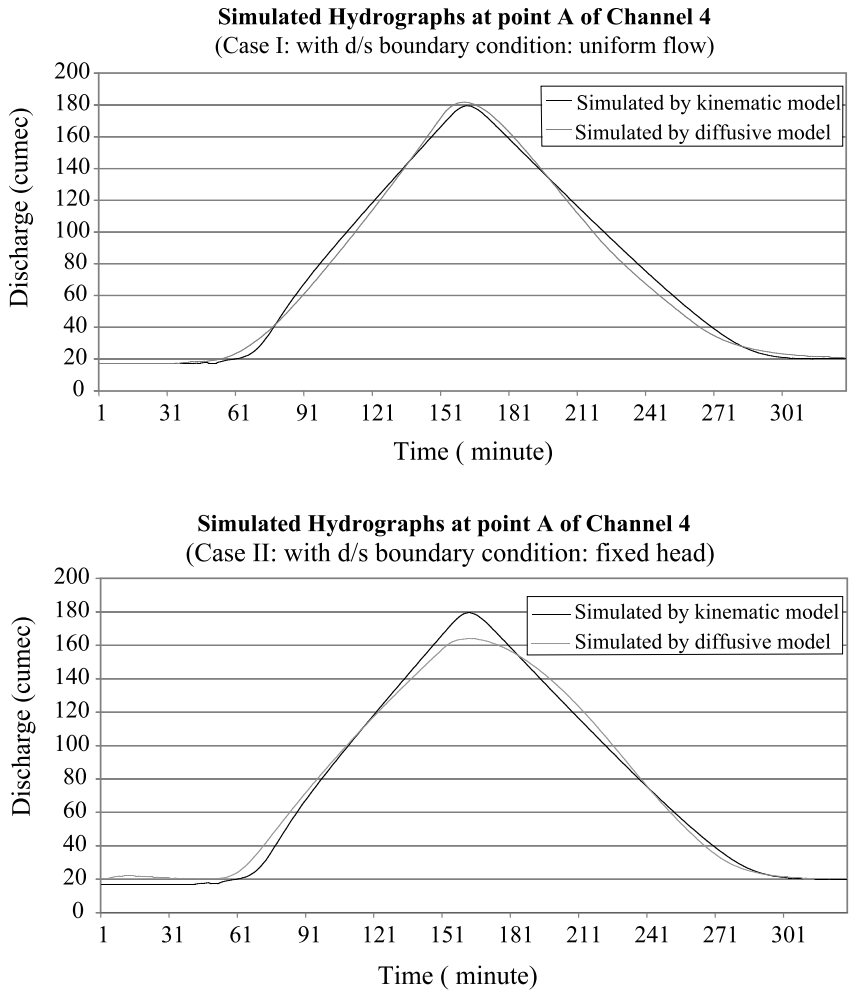

Figure 3. Comparison of simulated hydrographs at point A of channel 4 by kinematic and diffusive wave models considering uniform flow (Case I) and fixed head (Case II) as d/s boundary condition of channel 4

diffusive solution scheme is adequate for flood wave propagation simulation in channel networks taking into account the backwater effect.

2D Overland flow simulation model

Governing equations. Governing equations for 2D gradually varied unsteady flow can be derived from conservation of mass and momentum equations. Overland flow equations are the 2D expansion of 1D open channel flow Saint Venant's equations, which are written as:
Mass conservation equation (continuity equation):

$$\frac{\partial uh}{\partial x} + \frac{\partial vh}{\partial y} + \frac{\partial h}{\partial t} = q \tag{12}$$

Momentum Equations;
In X-direction:

$$\frac{\partial u}{\partial t} + u\frac{\partial u}{\partial x} + v\frac{\partial u}{\partial y} + g\left(\frac{\partial z}{\partial x} + S_{fx}\right) = 0 \tag{13}$$

In Y-direction:

$$\frac{\partial v}{\partial t} + u\frac{\partial v}{\partial x} + v\frac{\partial v}{\partial y} + g\left(\frac{\partial z}{\partial y} + S_{fy}\right) = 0 \tag{14}$$

Where, u and v are velocities of flow in X- and Y-directions, z is water head elevation from datum, and S_{fx} and S_{fy} are friction slopes in X- and Y-directions.

Friction slope can be evaluated using a uniform, steady-flow empirical resistance equation such as Chezy's or Manning's. Using Manning's equation,

$$S_{fx} = \frac{n_x^2 u^2}{h^{4/3}} \tag{15}$$

and,

$$S_{fy} = \frac{n_y^2 v^2}{h^{4/3}} \tag{16}$$

Where, n_x and n_y are Manning's roughness coefficients in X- and Y-directions and h is height of water head from surface.

Diffusive wave approximation. Neglecting the local convective acceleration terms in the X and Y momentum equations (first, second and third terms in Equations (13) and (14)), the momentum equations can be written in diffusive wave form as follows:

$$\frac{\partial h}{\partial x} = S_{ox} - S_{fx} \text{ in } X \text{ direction} \tag{17}$$

$$\frac{\partial h}{\partial y} = S_{oy} - S_{fy} \text{ in } Y \text{ direction} \tag{18}$$

Where, S_{ox} and S_{oy} are bed slopes in X- and Y-directions.
Combining Equations (15) with (17) and (16) with (18), yields

$$uh = \frac{1}{n_x}\left(S_{ox} - \frac{\partial h}{\partial x}\right)^{1/2} h^{5/3} \tag{19}$$

$$vh = \frac{1}{n_y}\left(S_{oy} - \frac{\partial h}{\partial y}\right)^{1/2} h^{5/3} \tag{20}$$

Replacing the above two relations in the mass balance equation of 2D surface flow, we obtain

$$\frac{\partial h}{\partial t} + \frac{\partial}{\partial x}\left[\frac{1}{n_x}\left(S_{ox} - \frac{\partial h}{\partial x}\right)^{1/2} h^{2/3} h\right] + \frac{\partial}{\partial y}\left[\frac{1}{n_y}\left(S_{oy} - \frac{\partial h}{\partial y}\right)^{1/2} h^{2/3} h\right] = q \tag{21}$$

As bed slopes in X- and Y-directions, S_{ox} and S_{oy} are known terms of surface elevation, Equation (21) is a function of variable h only.

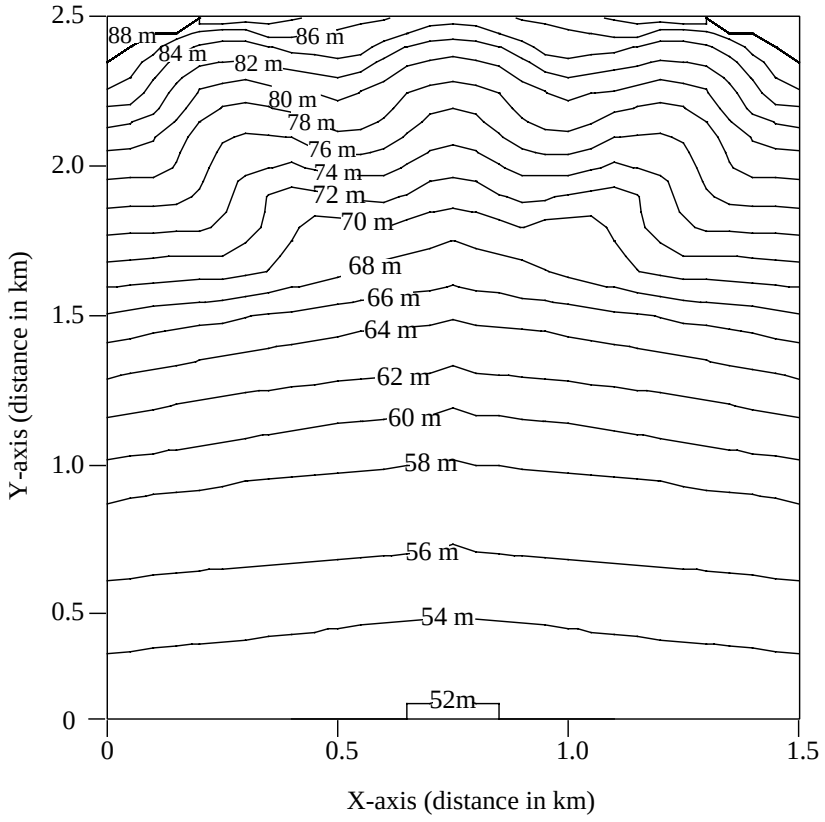

Figure 4. Contour map of elevation of the test area used for testing of overland flow simulation model

Solution scheme. An implicit finite difference scheme is used to solve the diffusive wave non-linear overland flow (Equation (21)) with the following assumptions.

1. First, non-linear terms of h, i.e. in terms $h^{2/3}$, $(S_{fx})^{0\cdot5}$ and $(S_{fy})^{0\cdot5}$, are considered explicitly, in the implicit solution scheme with Gauss-Seidal iteration using successive over relaxation (SOR) methods.
2. Then, non-linear terms are updated with the new head and iteration is done again to solve the whole equation implicitly to obtain final h for the next time step.

Testing of overland flow solution scheme. A hypothetical example data set is considered to test the validity and efficiency of the diffusive wave model for the simulation of flow in overland and a comparison with kinematic wave model has been made. The example data are of area 3·75 km^2 (1·5 km $\times$ 2·5 km) as shown in Figure 4 with roughness coefficients of 0·05. The boundary condition for all sides of the test area is considered as no flow boundary and hourly data of a rainfall event of 24-hour duration are added to the basin. The input rainfall event is shown in Figure 5. Both the kinematic and diffusive wave models are used to simulate overland flow propagation during the rainfall event for 24 hours with $dt = 1$ hour. The contours of the simulated surface heads at the end of the rainfall event obtained from the kinematic and diffusive wave models are shown in Figures 6(a) and 6(b). From the Figures, it can be seen that in the case of simulated contours by the diffusive wave model, water is accumulated in the lower part of the area as the boundary is a no flow boundary and spread around due to the backwater effect. However, in the case of the kinematic wave model, water is accumulated in the lowest elevation points and due to no consideration of the back water effect, water is not extended around. In two locations of the upper half of the test area, water accumulation is

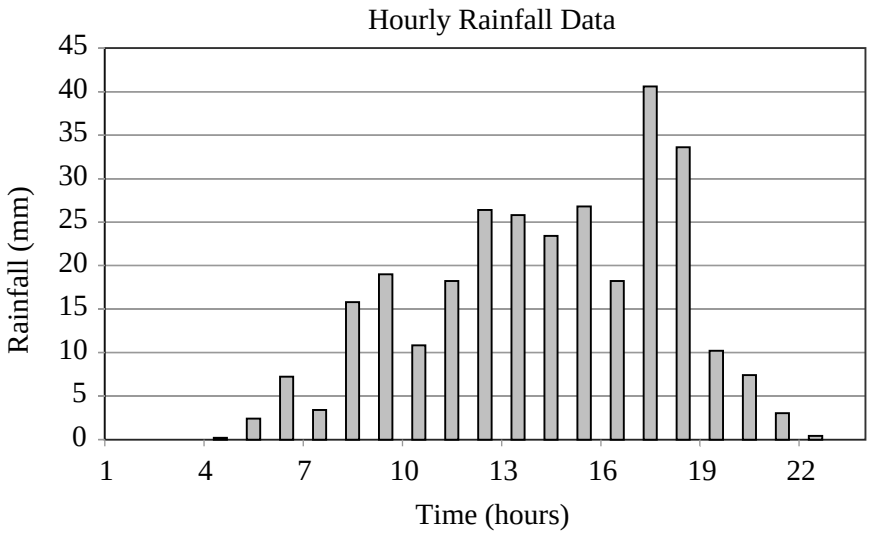

Figure 5. Input rainfall event used for testing of overland flow simulation model

seen in the simulation results of the kinematic wave model. These two areas have very flat bed slopes as can be easily seen from the contour map of elevation shown in Figure 4. Due to the very flat bed slopes, the downward movement of water is reduced in the kinematic wave model as it considers only bed slope for flow propagation, and thus water is accumulated. However, in case of the diffusive wave model, water movement is not reduced due to the small bed slope as it considers the energy slope in flow propagation. The results of the hypothetical example show that the diffusive model is adequate to simulate flood inundation as it can take into account the backwater effect.

Coupling of channel and overland flow models

The exchange of flow between the channel network and flood plains is simulated using the floodplain compartment concept (Fread, 1988; Inoue *et al.*, 1994). The floodplain compartments are surface grids along the river channels which are considered as boundary conditions in overland flow routing. Flow transfer between floodplain compartment and river is assumed to occur along Δx reaches which adjoin the river and floodplain compartments; this flow is assumed to be a broad-crested weir with submergence correction. Flow can be either away from the river or into the river, depending on the relative water surface elevations of the river and the floodplain compartment (Figure 7). The river water surface elevations are computed using the 1D diffusive wave model solution for channel network and the floodplain water surface elevations are computed by the 2D diffusive wave model for overland flows as described above. The exchange of flow between flood compartment and river reach in time step Δt is computed by a simple storage routing relation, i.e,

$$V_l^{t+1} = V_l^t + (I^{t+1} - O^{t+1})\Delta t$$

in which, V_l = volume of water in the floodplain compartment at time $t+1$ or t depending on the water elevation, I = inflow from the river grids to adjacent floodplain compartments, and O = outflow from the floodplain compartments to adjacent river grids. The broad-crested weir flow into or out of a single compartment is determined according to the following:

$$I = c_f s_b (h_r - h_w)^{3/2} \Delta L \quad \text{if } h_r > h_w \text{ and } h_r > h_{fp}$$
$$O = c_f s_b (h_{fp} - h_w)^{3/2} \Delta L \quad \text{if } h_{fp} > h_w \text{ and } h_{fp} > h_r$$

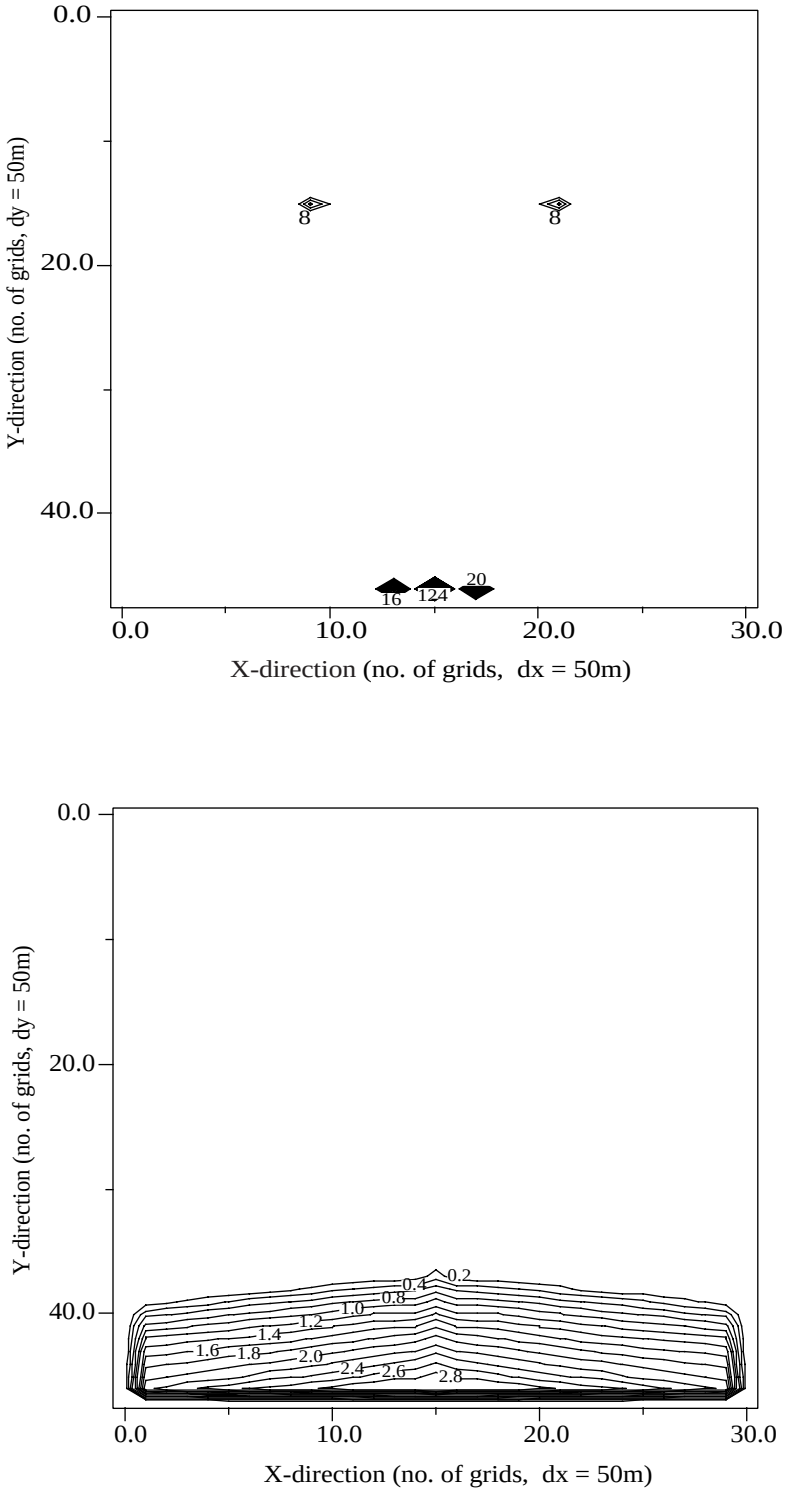

Figure 6. (a) Contours (in m) of surface water head as simulated by kinematic wave model; (b) contours (in m) of surface water head as simulated by diffusive wave model

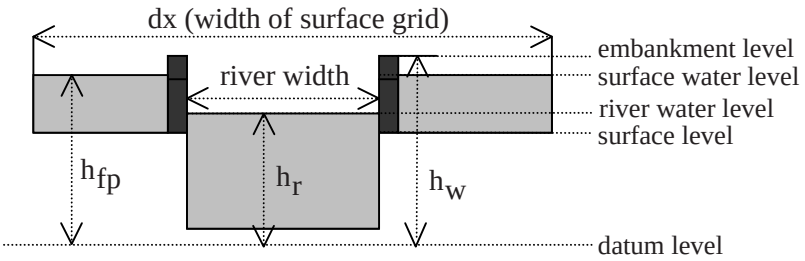

Figure 7. Concept of flow exchange between river and surface grids considering embankment heights

in which c_f = a specified discharge coefficient, h_r = the river water elevation from datum, h_{fp} = water surface elevation of the floodplain from datum, h_w = crest elevation of embankment from datum, ΔL = length of river reach, and s_b = submergence correction factor, i.e,

$$S_b = 1{\cdot}0 - 27{\cdot}8(H_r - 0{\cdot}67)^3 \quad \text{if } H_r > 0{\cdot}67$$
$$H_r = (h_r - h_w)/(h_{fp} - h_w) \quad \text{if } h_r > h_w \text{ and } h_r > h_{fp}$$
$$H_r = (h_{fp} - h_w)/(h_r - h_w) \quad \text{if } h_{fp} > h_w \text{ and } h_{fp} > h_r$$

Coupling of channel network and overland flow simulation models with other components

The newly developed combined channel network and overland flow simulation model is coupled with other components of IISDHM such as (1) evapotranspiration, (2) unsaturated zone, and (3) saturated zone modules, to develop a complete distributed hydrologic model for flood simulation. The flow chart in Figure 8 shows the concept of coupling. Common blocks in Fortran code are used to formulate the algorithm for coupling the different flow simulation modules at a specified time interval.

MODEL APPLICATION

Study area

The study area selected for model application is a moderate size basin, named Ichinomiya river basin, with an area of 220 km^2, located in Chiba prefecture, Japan between latitude 35°18′N to 35°30′N and longitude 140°10′E to 140°25′E as shown in Figure 9. The topography of the basin varies from hilly areas in the western part with maximum elevation of about 155 m to lowland flat areas in the eastern part with minimum elevation of about 1 m from mean sea level. The mean annual rainfall is approximately 1,700 mm and rainfall distribution is almost uniform in the entire basin.

Data preparation

A vast amount of temporal and spatial data is required as input data for using a physically based distributed hydrologic model for any hydrologic process simulation as shown in Table II. In this study, GIS is extensively used for the processing of various spatial data layers required for simulation. The following two sub-sections describe details of availability and the gathering of temporal and spatial data for the study area and the processing of spatial data.

Temporal data. There are a total of five rainfall gauging stations in the Ichinomiya basin, where data are recorded in hourly intervals (refer to Figure 9); one station is maintained by AMEDAS and the other four are maintained by the river department of the local city offices. River water level is measured in hourly intervals in two water level gauging stations in the Ichinomiya river. Daily pan evaporation is measured in one station. Available time series data of rainfall, pan evaporation and river water level are collected from the

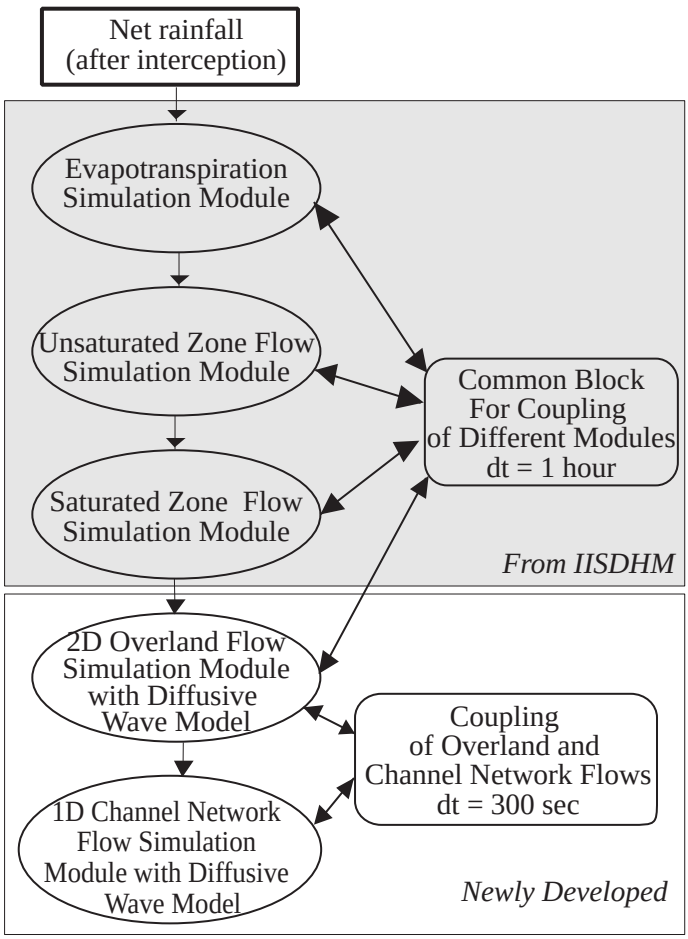

Figure 8. Concept of coupling of different modules of distributed hydrologic model

Table II. List of required temporal and spatial input data for a distributed hydrologic model

Hydrologic component	Data required	
	Time series data	Spatial and other data
Surface and river flow	Rainfall Water level/discharge (*for model verification*)	Topography data Locations of hydrometeorologic stations Drainage network Detention storage Surface roughness coefficient
Evapotranspiration	Potential evaporation Leaf Area Index and Root Distribution Function for each landcover pattern	Landcover distribution
Unsaturated zone flow		Soil type distribution Hydrogeological properties of each soil type
Saturated zone flow	Groundwater abstractions data and location of abstraction wells	Distribution of geological layers and upper and lower levels of each layer Hydrogeological parameters of each layer

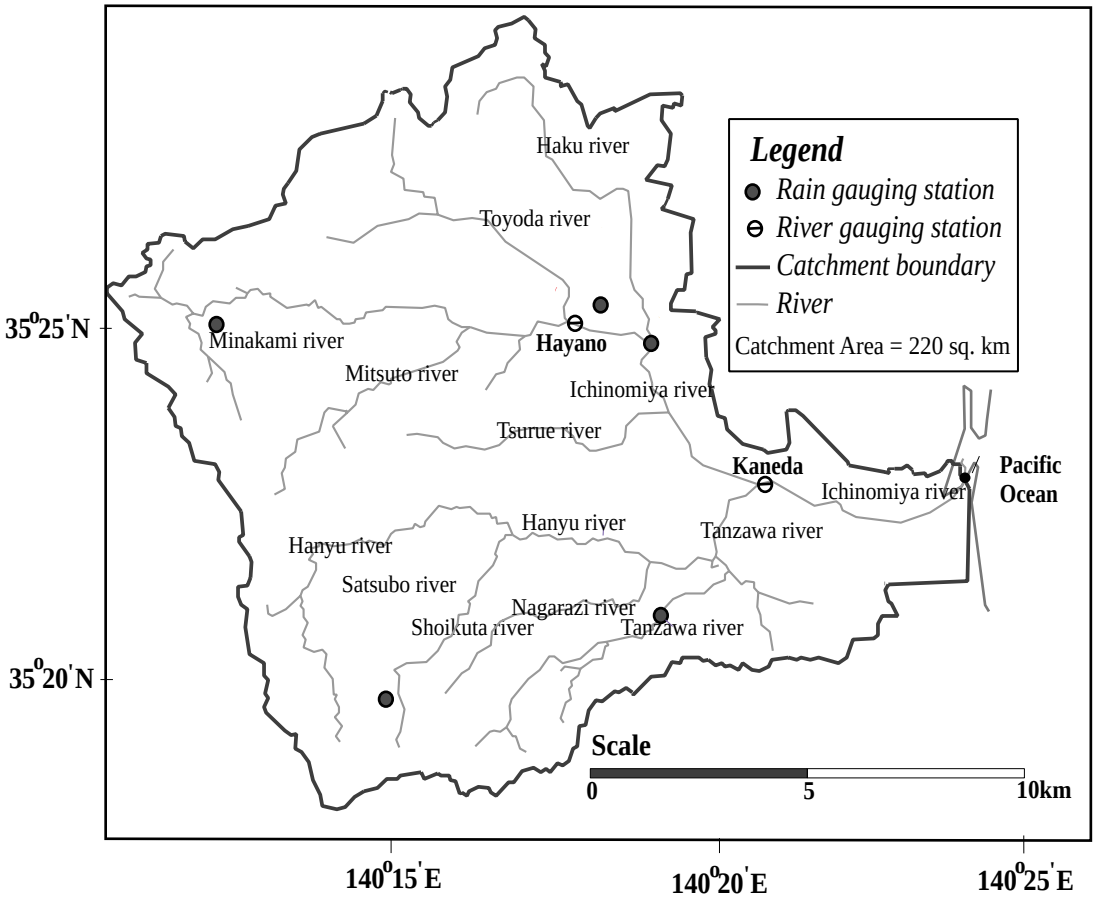

Figure 9. Ichinomiya river basin with locations of hydrometeorological gauging stations

data bank of the responsible authorities. Daily evaporation data for the other stations are estimated from windspeed, sunshine, temperature data available for the three rainfall gauging stations. For spatial distribution of time series data, the thiessen polygon concept is used. Monthly data of leaf area indices and root distribution functions for different landcover patterns are obtained from available reports.

Spatial data.

DEM and river network: DEM (Digital Elevation Model) of the study area was generated from 50 m grid elevation data that were obtained from Japan Map Center. The river network was delineated from the DEM using the methodology of Tarboton *et al*. (1991). However, the generated river system was not following the actual river path, and hence, the original DEM was modified with additional 1 m interval contour data obtained from a 1 : 2500 scale map for the lower flat area of the basin and the river network was generated again. The final generated river network used in the flood simulation is shown in Figure 10 together with the actual river network as obtained from ground truth data. Except for the lower flat areas, the generated river network matches well with the actual flow path.

River parameters: Cross-sections and bed profiles of all the major rivers of the basin were obtained from the river department of the local city offices. Along the Ichinomiya river, earthen embankments exist on both sides of the river, which were built for flood protection. The elevations of river embankment and bed profile

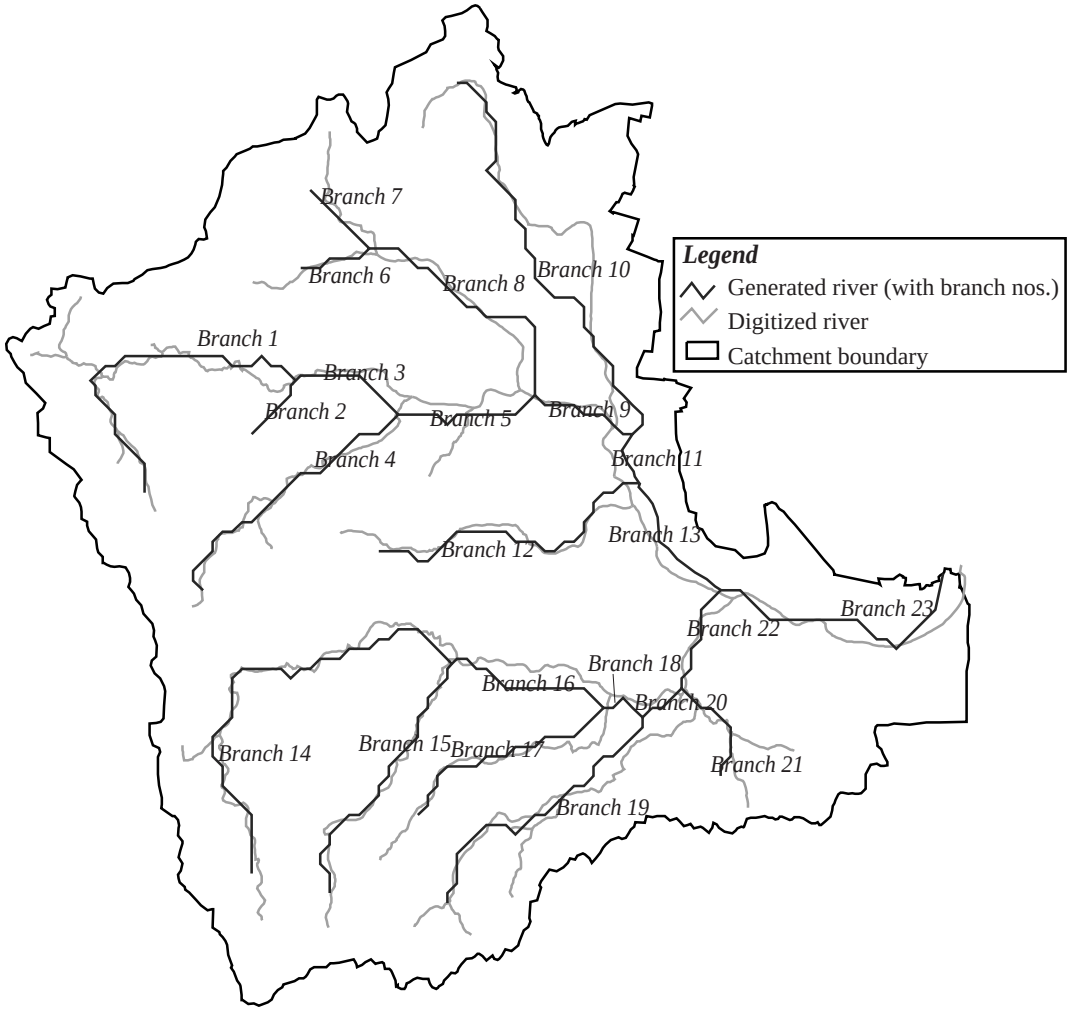

Figure 10. Generated and actual river network of the Ichinomiya river basin

of the Ichinomiya river from d/s to u/s are shown in Figure 11. In the model, average embankment heights in all the river points are incorporated. However, during the flow exchange between surface and river, embankment height is considered for calculation of inflow from river grids to adjacent floodplain compartment only. In the calculation of outflow from surface grid to river, embankment height is neglected as it has no effect on water movement from surface to river due to available drainage pipes which are constructed for releasing water from surface to river.

Landcover and surface roughness: There are a total of six major landcover classes within the study area, which are forest, paddy, light grass, vegetable, water body and urban area. SPOT satellite data of 20 m pixel size of 7 October 1996 were used to derive detailed landcover patterns in the study area. The classified landcover map is shown in Figure 12. Surface roughness coefficients were used according to the landcover pattern as shown in Table III.

Soil classes and parameter estimation: A soil map was obtained from the Mitsui Consultant Co., Ltd., Tokyo, which has six major soil classes. To determine the hydrologic parameters required for distributed hydrologic

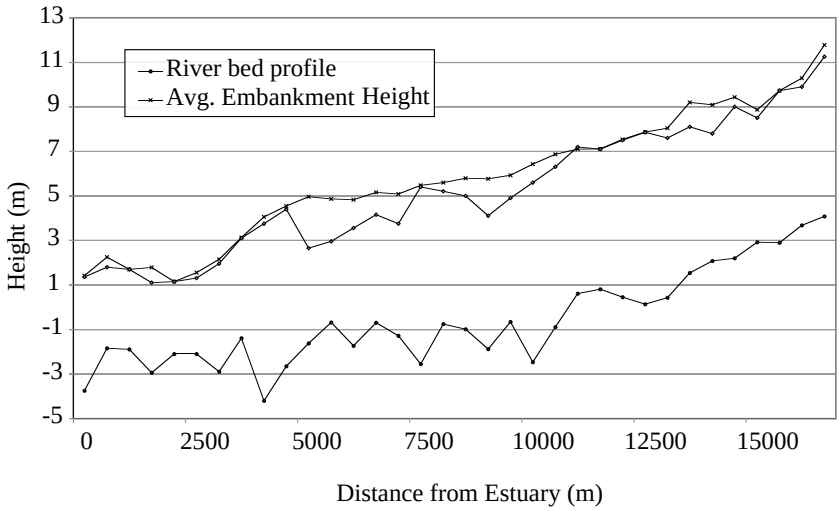

Figure 11. River bed profile and embankment heights along the Ichinomiya river from downstream to upstream

Table III. Manning roughness coefficients of different landcover patterns

Landcover pattern	Manning roughness coefficient
Light forest	0·07
Dense forest	0·10
Agriculture	0·04
Water body	0·03
Grass land	0·05
Urban	0·02

model, constant head in-situ soil tests were conducted in the Ichinomiya basin during 6–7 August 1997 in some selected sites. Soil parameters were computed using the methodology developed by Herath *et al*. (1990) from the field measurement data. Laboratory tests were conducted to derive the soil-moisture retention curves for different soil types using soil samples collected from the field for different sites and layers.

Aquifer data and groundwater table: In the study area, a single unconfined aquifer is recognized by geophysical logging correlation and depth which varies from 5 to 10 m in the lower part of the basin; below that bedrock exists. The groundwater table is very shallow, just about 3 to 5 m below the surface. Borehole data and groundwater tables data were supplied by the Mitsui Consultant Co., Ltd., Tokyo for some sites, and available data were interpolated to develop the spatial data of aquifer depth and initial groundwater table.

Flood inundation simulation

Upstream and downstream conditions for river channels: The channel network considered in the model has a total of 23 branches (refer to Figure 10). Out of that, 12 branches have free u/s ends and one has a free d/s end, i.e., the outlet of the river basin, which require boundary conditions to obtain a sufficient number of equations to solve the channel network algorithm. There was no data available in the u/s ends of these branches and as all these u/s ends are located in hill slopes, u/s boundary conditions for all the branches are considered as fixed head boundary. The hourly data of seawater level measured in the estuary of the Ichinomiya river is considered as the d/s boundary condition at the outlet of the river basin as shown in Figure 13. From 22–23 September 1996, the basin suffered from a flood disaster due to heavy rainfall caused

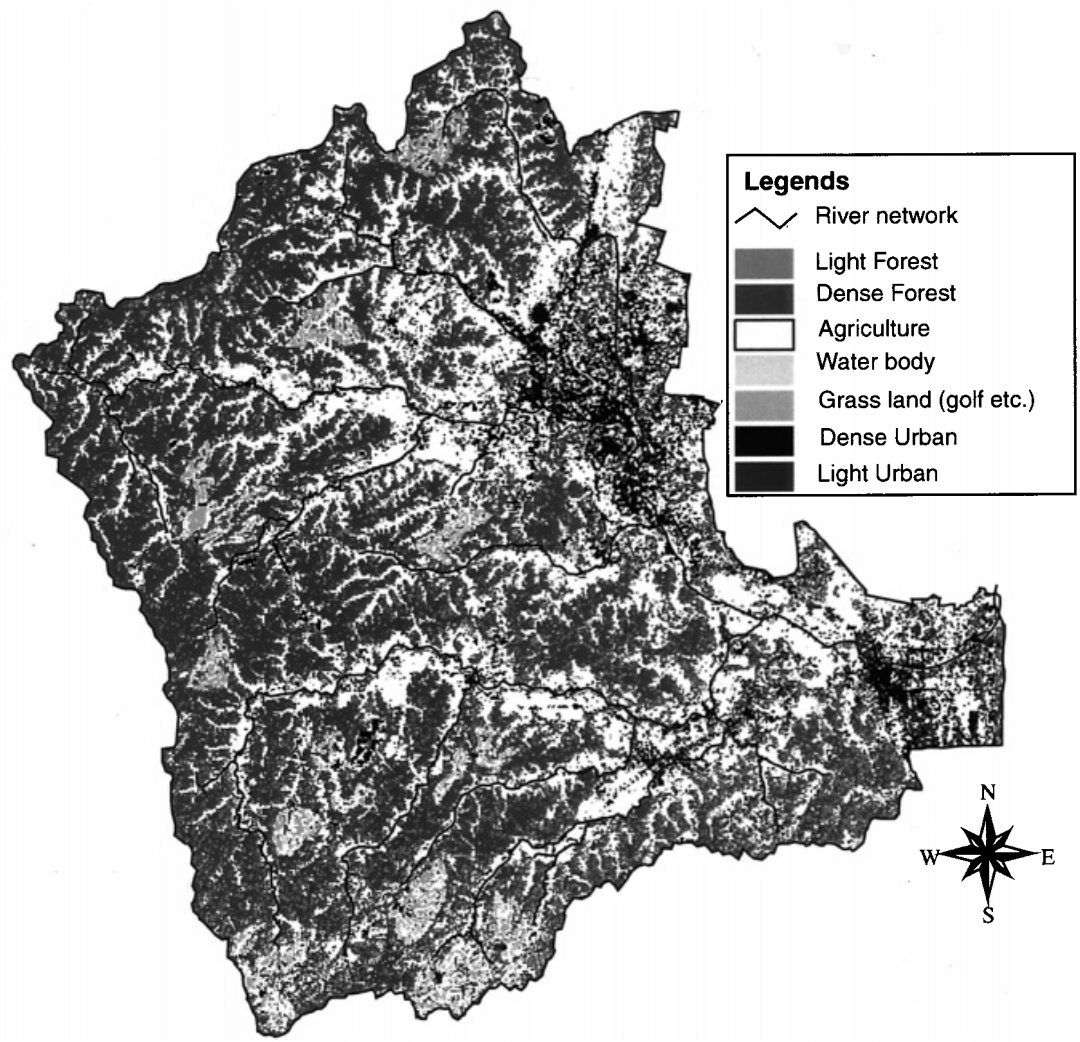

Figure 12. Landcover map of the Ichinomiya river basin as classified from SPOT XS sensor data of 20 m pixel resolution

by Typhoon 17. Within 24 hours between 21–22 September the whole basin received about 360 mm rainfall. The distributed hydrologic model was used to simulate this flood event. The model was run for a period of four days starting from 20 September, two days before the typhoon passed through the basin. As the input rainfall data was of hourly resolution, coupling time for different modules of the model was selected as one hour except for surface and river modules. Coupling time between surface and river modules was taken as 300 sec. to avoid any numerical instability in the simulation. Figure 14 shows the basin average rainfall during the period of simulation.

Interpretation of simulated results

Flood hydrographs: Figures 15 and 16 show the comparison of simulated flood hydrographs with observed hydrographs at the gauging stations Hayano and Kaneda (refer to Figure 9). The simulated hydrograph matches very well with the observed discharge hydrograph at Hayano station. At Kaneda station, the simulated flood hydrograph matches quite well with the observed hydrograph except during the peak flow. The simulated peak of the discharge at the Kaneda station is higher than the observed discharge.

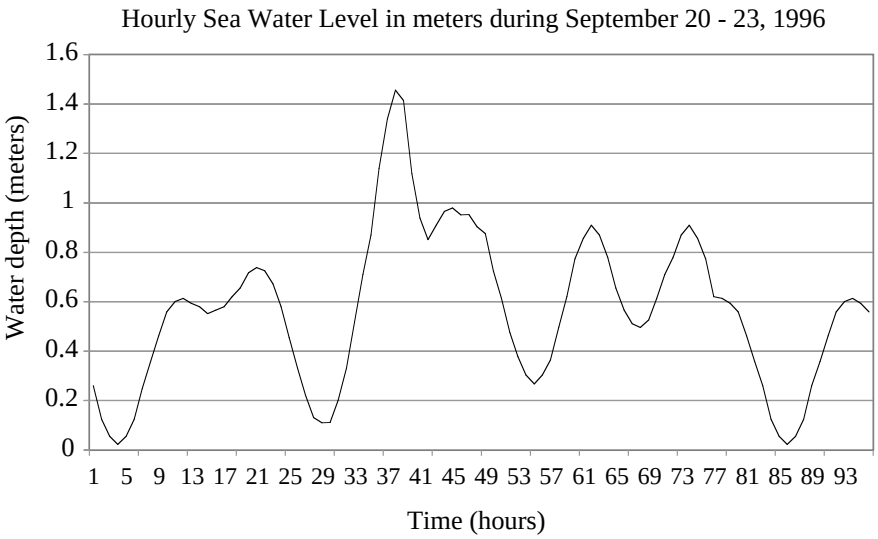

Figure 13. Hourly sea water level data measured in the estuary of Ichinomiya river during the period of simulation

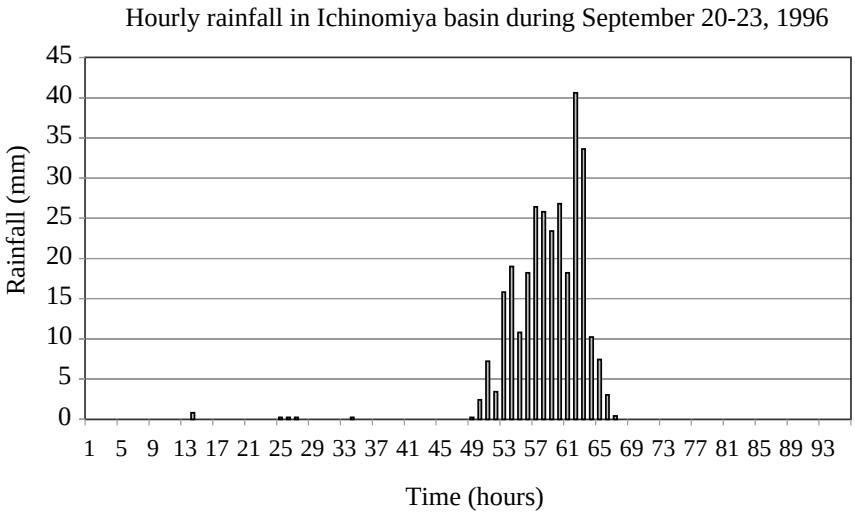

Figure 14. Basin average rainfall during the period of simulation

Flood inundation: Figure 17 shows the simulated flood inundation with flood water depths in the basin. The simulated flood extent is the maximum extent of the flooded area with flood water height above 0·4 m that was observed at 16:00 on 22 September 1996. Figure 18 shows the flood extension as surveyed by the Ministry of Construction, Japan. By comparing the simulated results with the surveyed flood extent, it can be said that simulated result is close to the actual situation. It can be noticed that there is some shifting of the simulated flood inundation from the surveyed one. This is mainly due to the difference between the actual channel network and the generated channel network from the DEM, which was used for simulation. It is seen from Figure 10 that the generated river network does not match well with the actual flow paths in the lower part of the basin. As most of the flooded areas are along the rivers, simulated flooded areas are also shifting from the original locations along with the river network. Also, the simulated flood extension is larger than the observed flooded areas. This may be due to road networks that worked as embankments in many

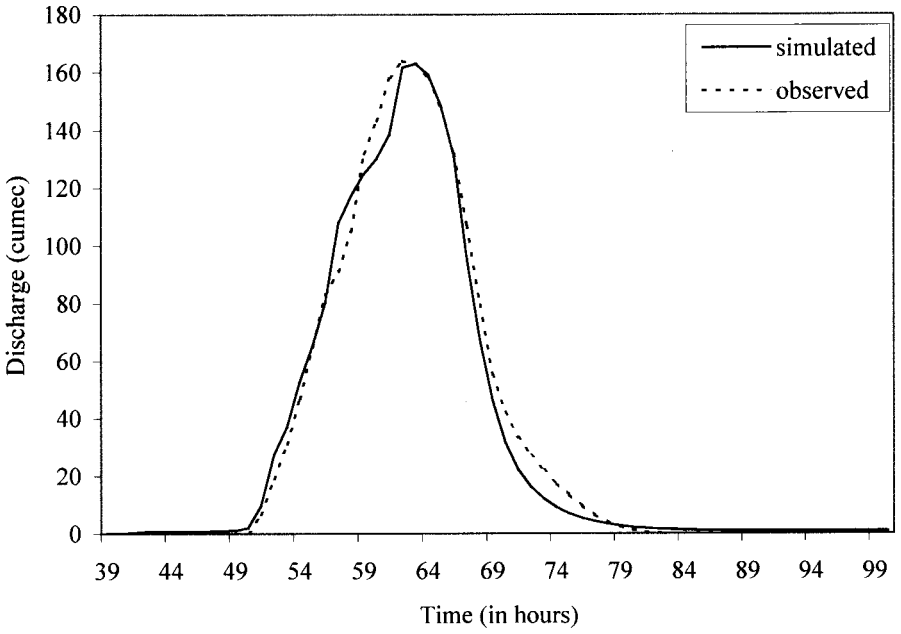

Figure 15. Comparison of simulated and observed discharge hydrographs in Hayano station

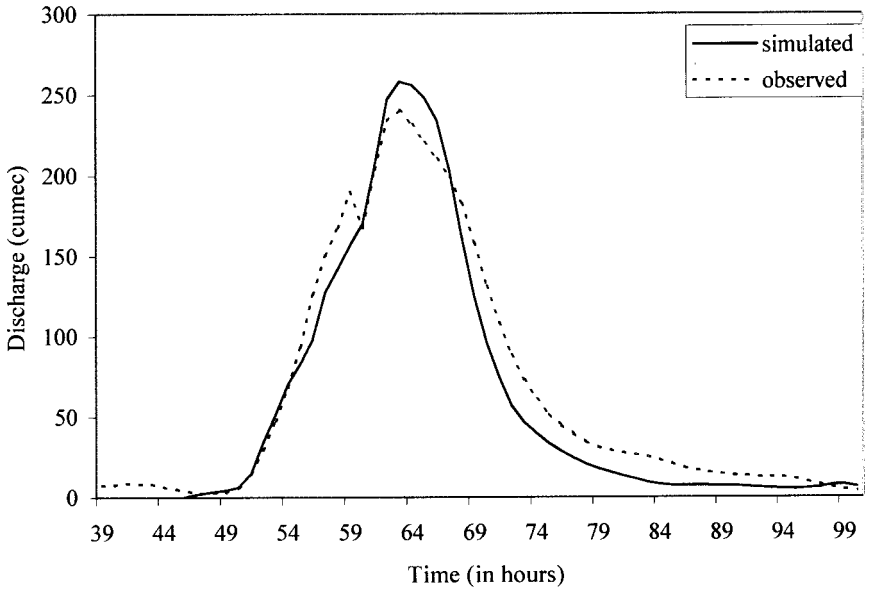

Figure 16. Comparison of simulated and observed discharge hydrographs in Kaneda station

areas preventing the movement of flood water from river sides, as suggested by local city officials. The road networks are not separately considered in the model, at present.

No embankment was breached by this flood. However, flood water overtopped embankments in many places along Ichinomiya river. Figure 19 shows the locations of embankment overtopping with maximum

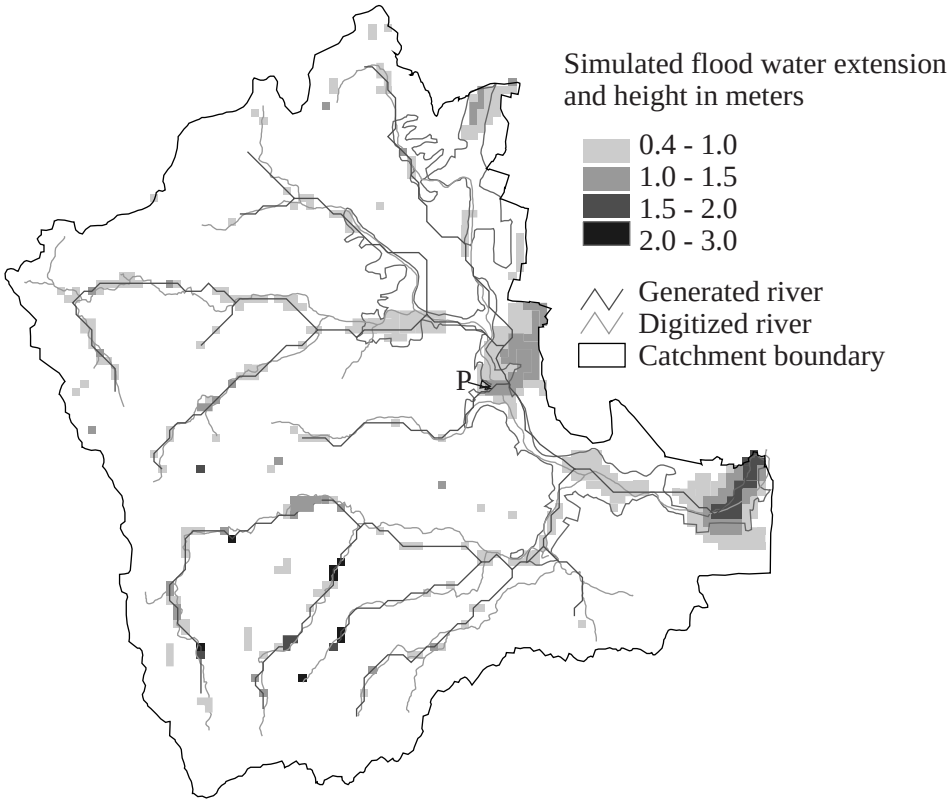

Figure 17. Simulated spatial extent of flood inundation and flood water height in the Ichinomiya basin

flood water height and embankment elevation and bed profiles along Ichinomiya river as obtained from simulation at 16:00 on 22 September 1996.

Figure 20 shows the temporal variation of flood water height at the location *P* of Mobara ward (refer to Figure 17) during the flood period and Figure 21 shows the maximum height of flood water (1·6 m) at the same location as obtained from the questionnaire survey conducted by the Ministry of Construction. The maximum height of simulated flood water is very close to the surveyed data.

Evaporation and infiltration: Figure 22 shows the total water balance in the basin during the simulation period. From this result, it can be seen that the interception and evapotranspiration components are not very high in this case. However, infiltration is relatively large. This shows that infiltration reduces the amount of surface water and thus, has an impact on flood water height and extent.

CONCLUSIONS

An integrated distributed model was developed in this study by combining a newly developed coupled overland and channel network flow simulation model with other components of IISDHM. The river and surface models were individually verified with test data set. The model was applied to simulate a flood event in a Japanese river basin to verify its applicability in basin scale flood simulation.

The simulated flood hydrographs show good agreement with observed data. The backwater effect in the lower part of the river is well represented by the simulated results. The model has successfully simulated the flood inundation in a basin scale considering all heterogeneity of physical characteristics of the basin. Although the simulated flood inundation results do not perfectly match observed data, they are close to

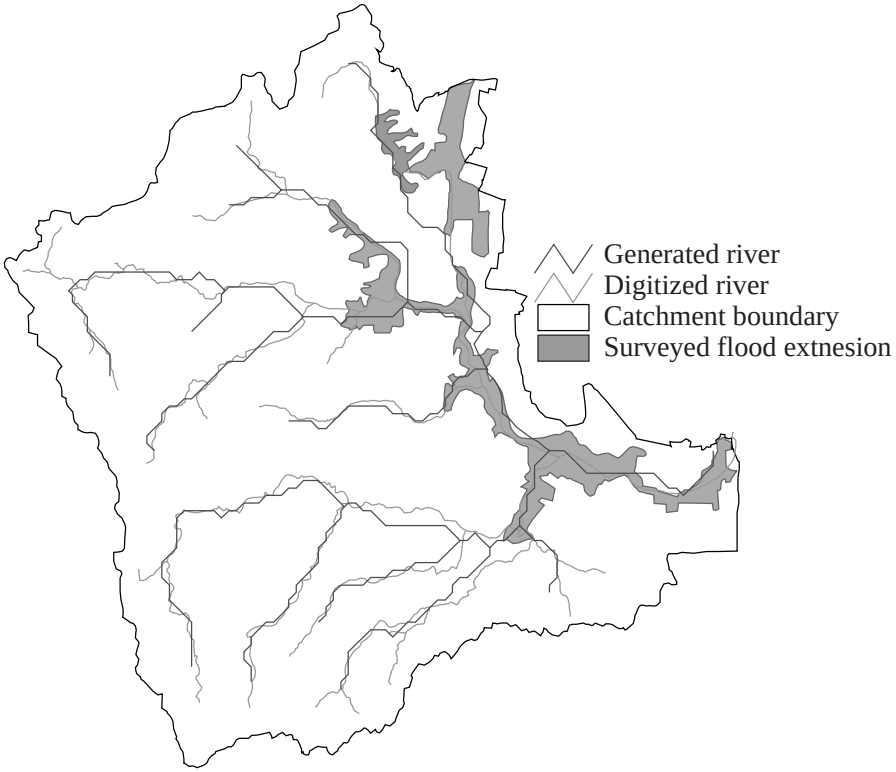

Figure 18. Flood extension in the Ichinomiya basin due to Typhoon 17 in September 1996 as surveyed by the Ministry of Construction, Japan

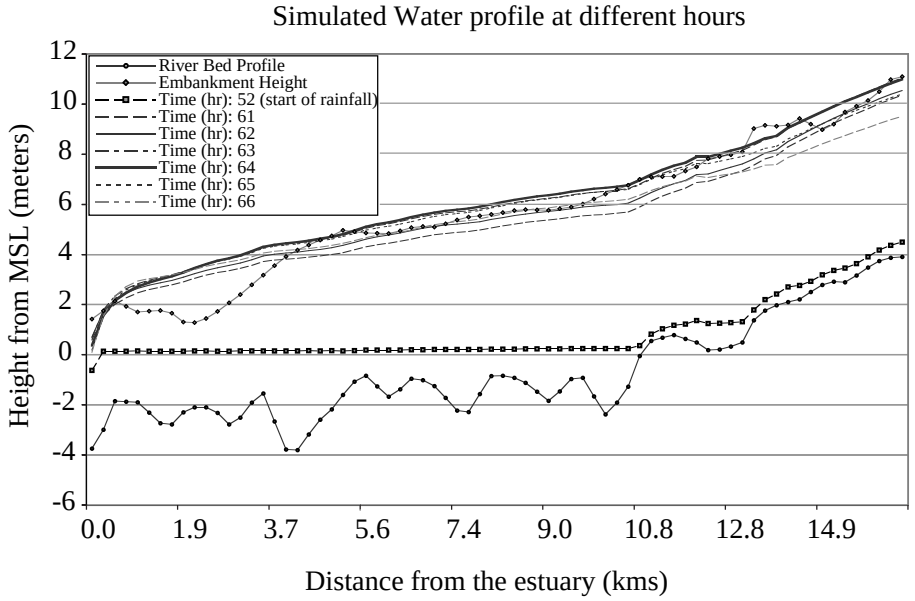

Figure 19. Flood water heights along the Ichinomiya river at different hours during peak flow as obtained from the simulation together with the embankment elevations and bed profile

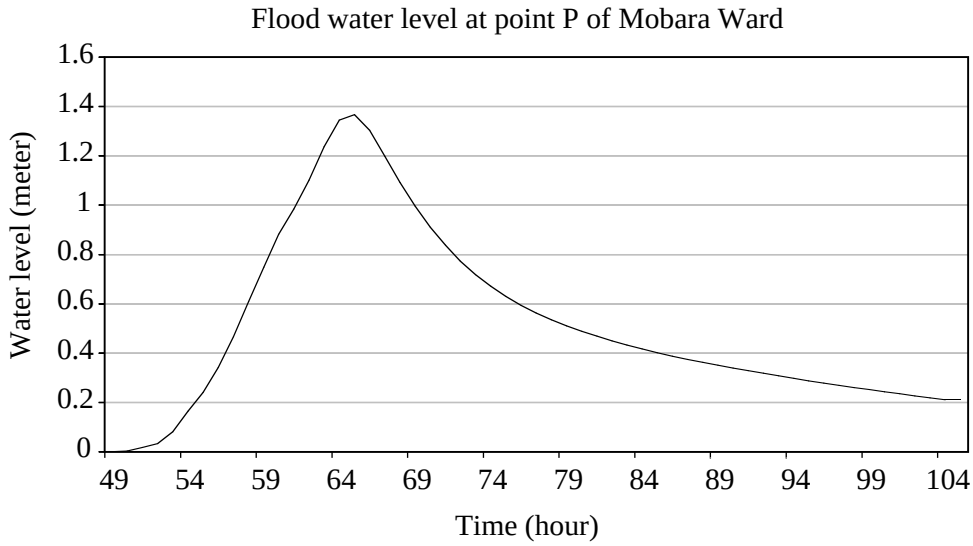

Figure 20. Temporal variation of flood water height during the rainfall event caused by Typhoon 17 at location P of Mobara Ward

Figure 21. Maximum height of flood water at point P of Mobara Ward as observed by Local City Office personnel during questionnaire survey conducted several days after recession of flood water

surveyed flood inundation. It is possible to improve the model outcome with the improvement of input spatial parameters and with certain modifications such as the incorporation of road network, etc. From this study, it can be concluded that the physically based distributed hydrologic models with detailed catchment information can be used for flood inundation simulations at basin scale. The model results show that there is some impact of evapotranspiration and infiltration in surface and river flows. It is necessary to consider these components together with surface and river models for getting accurate results in flood simulation.

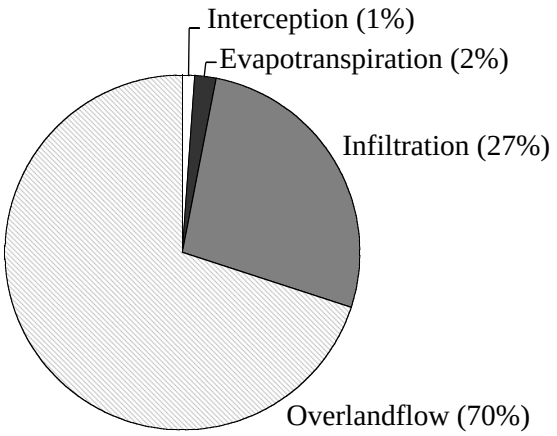

Figure 22. Total water balance in the basin during the four-day period of simulation

The physically based distributed hydrologic model developed in this study is a relatively new approach for basin scale flood inundation simulation considering all the components of the hydrologic cycle. The methodology has a wide range of applications in many practical problems such as flood disaster mitigation works, river training work improvement, real time flood inundation modelling, flood damage estimation, etc.

ACKNOWLEDGEMENT

The authors gratefully acknowledge the contribution to this study by the Mitsui Consultant Co., Ltd., Tokyo, who provided all the base data for model application.

REFERENCES

Akan AO, Yen BC. 1981. Diffusive-wave flood routing in channel networks. *Journal of the Hydraulics Division, ASCE* **107**(HY6), 719–731.

Cui G, Williams B. 1998. Downstream characteristic Lagrangian hybrid method for flows in open channels. *Journal of Hydraulic Research* **36**: 379–396.

Fennema RJ, Chaudhry MH. 1989. Implicit methods for two-dimensional unsteady free-surface flows. *Journal of Hydraulic Research* **27**: 321–332.

Field WG, Lambert MF, Williams BJ. 1998. Energy and momentum in one dimensional open channel flow. *Journal of Hydraulic Research* **36**: 29–42.

Fread DL. 1988. The NWS DAMBREAK model: Theoretical background/user documentation. National Weather Service (NWS), NOAA: Silver Spring, Maryland.

Gee DM, Anderson MG, Baird L. 1990. Two-dimensional floodplain modeling. *In Hydraulic Engineering, Proceedings of the 1990 National Conference*, Hydraulic Division, ASCE: Boston, MA; 773–778.

Herath S, Hirose N, Musiake K. 1990. A computer package for the estimation of infiltration capacities of shallow infiltration facilities. *Proceedings of the Fifth International Conference on Urban Storm Drainage*; 111–118.

Inoue K, Nakagawa H, Toda K. 1994. Numerical analysis of overland flood flows by means of one- and two-dimensional models. *Proceedings of the 5th JSPS-VCC Seminar on Integrated Engineering 'Engineering Achievement and Challenges'*, DRPI, Kyoto University: Kyoto, Japan; 388–397.

Iwasa Y, Inoue K. 1982. Mathematical simulations of channel and overland flood flows in view of flood disaster engineering. *Natural Disaster Science* **4**: 1–30.

Jha R, Herath S, Musiake K. 1997. Development of IIS distributed hydrological model (IISDHM) and its application in Chao Phraya river basin, Thailand. *Annual Journal of Hydraulic Engineering, JSCE* **41**: 227–232.

Rahman M, Chaudhry MH. 1997. Computation of flow in open-channel transitions. *Journal of Hydraulic Research* **35**: 243–256.

Samules PG. 1985. Modeling of river and floodplain flow using the finite element method. *Hydraulic Research*, Technical Report No. SR61: Wallingford, UK.

Tarboton DG, Bras RL, Rodreguez-Iturbe I. 1991. On the extraction of channel networks from digital elevation data. *Hydrological Processes* **5**: 81–100.

Zhang W, Cundy TW. 1989. Modeling of two-dimensional overland flow. *Water Resources Research* **25**: 2019–2035.

